





RNA-seq Analysis of Peri-Implant Tissue Shows Differences in Immune, Notch, Wnt, and Angiogenesis Pathways in Aged Versus Young Mice

Kathleen Turajane,¹ Gang Ji,^{1,2} Yurii Chinenov,^{1,3} Max Chao,^{1,3} Ugur Ayturk,¹  Vincentius J Suhardi,¹ 
Matthew B Greenblatt,^{1,4}  Lionel B Ivashkiv,^{1,3} Mathias PG Bostrom,¹ and Xu Yang¹ 

¹Hospital for Special Surgery, New York, NY, USA

²The Third Hospital of Hebei Medical University, Shijiazhuang, China

³David Z. Rosensweig Genomics Research Center, Hospital for Special Surgery, New York, NY, USA

⁴Department of Pathology and Laboratory Medicine, Weill Cornell Medicine, New York, NY, USA

ABSTRACT

The number of total joint replacements (TJR) in the United States is increasing annually. Cementless implants are intended to improve upon traditional cemented implants by allowing bone growth directly on the surface to improve implant longevity. One major complication of TJR is implant loosening, which is related to deficient osseointegration in cementless TJRs. Although poor osseointegration in aged patients is typically attributed to decreased basal bone mass, little is known about the molecular pathways that compromise the growth of bone onto porous titanium implants. To identify the pathways important for osseointegration that are compromised by aging, we developed an approach for transcriptomic profiling of peri-implant tissue in young and aged mice using our murine model of osseointegration. Based on previous findings of changes of bone quality associated with aging, we hypothesized that aged mice have impaired activation of bone anabolic pathways at the bone-implant interface. We found that pathways most significantly downregulated in aged mice relative to young mice are related to angiogenic, Notch, and Wnt signaling. Downregulation of these pathways is associated with markedly increased expression of inflammatory and immune genes at the bone-implant interface in aged mice. These results identify osseointegration pathways affected by aging and suggest that an increased inflammatory response in aged mice may compromise peri-implant bone healing. Targeting the Notch and Wnt pathways, promoting angiogenesis, or modulating the immune response at the peri-implant site may enhance osseointegration and improve the outcome of joint replacement in older patients. © 2021 The Authors. *JBMR Plus* published by Wiley Periodicals LLC on behalf of American Society for Bone and Mineral Research.

KEY WORDS: AGING; CELL/TISSUE SIGNALING – PARACRINE PATHWAYS; IMPLANTS; MOLECULAR PATHWAYS – REMODELING; PRECLINICAL STUDIES

Introduction

The number of total joint replacements (TJR) in the United States is increasing annually, including increased utilization in elderly patients well into the eighth or even ninth decade of life.⁽¹⁾ Cementless implants are intended to overcome the shortcomings of traditional cemented implants by allowing bone growth directly onto their surface to improve implant longevity.^(2,3) Although most patients have good long-term outcomes, a major complication of TJR is implant loosening,^(4,5) which in cementless TJRs is related to deficient osseointegration, the physical and functional connection between bone and implant.^(6,7) One of the most important risk factors for poor osseointegration, and thus decreased implant longevity, is elder age of patients.⁽⁸⁾ Poor osseointegration in aged patients is

typically attributed to decreased basal bone mass.^(9,10) Little is understood about the mechanisms that compromise de novo bone formation—bone ingrowth into porous titanium implants in the elderly. To develop therapeutic strategies to improve clinical outcome of TJRs in elderly patients, we need to understand how aging compromises the molecular pathways important for osseointegration.

TJR surgery involves creation of a bone injury by drilling a canal into bone, followed by implant insertion and subsequent healing and ingrowth of cancellous bone into the porous surface of the titanium implant.⁽¹¹⁾ We and others have developed animal models to analyze the process of orthopedic implant integration.^(12–24) In our mouse model, load-bearing titanium implants inserted into the proximal tibia become integrated with the surrounding bone over a 4-week period.^(15,19,23) Little is known

This is an open access article under the terms of the Creative Commons Attribution License, which permits use, distribution and reproduction in any medium, provided the original work is properly cited.

Received in original form April 28, 2021; revised form July 19, 2021; accepted July 27, 2021.

Address correspondence to: Xu Yang, MD, Hospital for Special Surgery, 535 East 70th Street, New York, NY 10021, USA. E-mail: yangx@hss.edu

JBMR[®] Plus (WOA), Vol. 5, No. 11, November 2021, e10535.

DOI: 10.1002/jbm4.10535

© 2021 The Authors. *JBMR Plus* published by Wiley Periodicals LLC on behalf of American Society for Bone and Mineral Research.

about molecular pathways that regulate this process. In other bone injuries such as fracture, repair initiates with a hematoma and an inflammatory phase followed by a bone formation phase whose mechanism (endochondral versus intramembranous) is determined by the extent of mechanical stability at the injury site. The determinants of effective bone repair include the nature, magnitude, and kinetics of the inflammatory response, effective neovascularization, the functionality and mobilization of skeletal progenitor cells and osteoclasts, and induction of the canonical Wnt, bone morphogenetic protein (BMP), and Notch anabolic pathways.^(25,26) Little is known about the relative importance of these determinants in implant osseointegration.

Cross-regulation between the immune system and bone metabolism has long been appreciated and its study has been termed “osteimmunology.”^(27,28) Sustained high-level inflammation associated with infection, autoimmune diseases, and foreign body reactions induces pathological bone resorption. Important mechanisms include augmentation of osteoclastogenesis directly by macrophage-derived inflammatory cytokines such as IL-1 and TNF, and indirectly by Th17 T cells via activation of stromal cells to express receptor activator of NF-κB ligand (RANKL).^(29,30) Th17 cells are expanded and promote bone resorption in response to continuous elevation of parathyroid hormone (PTH).⁽³¹⁾ Under inflammatory conditions, cytokines such as TNF and IFN-γ additionally suppress bone formation by inhibiting the differentiation and function of osteoblasts.⁽³²⁾

Immune-bone cross-talk is also important in the absence of overt inflammatory disease and can play important roles in bone homeostasis, response to injury, and subsequent repair.^(27,28) An early, transient, low-level inflammatory response after bone fracture is mediated by inflammatory cytokines, including TNF and IL-17, and is important for removal of dead cells and tissue debris and priming of subsequent neovascularization and mobilization of PDGFRα+Sca1+ skeletal progenitors.^(33,34) The later phases of bone healing are promoted by trophic (also termed M2)

macrophages that produce growth factors and suppressed by IFN-γ-producing CD8+ T cells.^(35–38) Additionally, bone healing and repair can be promoted by regulatory T cells (Tregs) that suppress pathogenic functions of CD8+ T cells and instead induce these cells to produce Wnt10b in the bone marrow.^(36,39) The overall model is that a balanced inflammatory response that evolves over time from type 1 inflammatory to type 2 pro-resolution immunity can promote bone healing, whereas excessive or unbalanced immune responses will delay and compromise repair.

Here, we sought to identify pathways important for osseointegration that are compromised by aging. In this study, we developed an approach to perform transcriptomic profiling of peri-implant tissue in young and aged mice using our murine model of osseointegration.⁽²³⁾ We hypothesized that aged mice have impaired activation of bone anabolic pathways at the bone-implant interface. We found that pathways most significantly downregulated in aged relative to young mice are related to angiogenesis, Notch, and Wnt signaling. This downregulation of bone formation pathways was associated with strikingly increased expression of inflammatory and immune genes at the implant-bone interface in aged mice. These results identify osseointegration pathways affected by aging and suggest that an increased inflammatory response in aged mice may compromise bone healing.

Materials and Methods

Study design

Using an IACUC-approved protocol, 16-week-old (young) and 91-week-old (aged) female C57BL/6 mice ($n = 10$ per group) were purchased from Jackson Laboratory (Bar Harbor, ME, USA). A porous titanium (Ti6Al4V) implant (Eosint M 270; Eos Electro Optical Systems, Munich, Germany) was inserted into the right proximal tibia of the mice as previously described

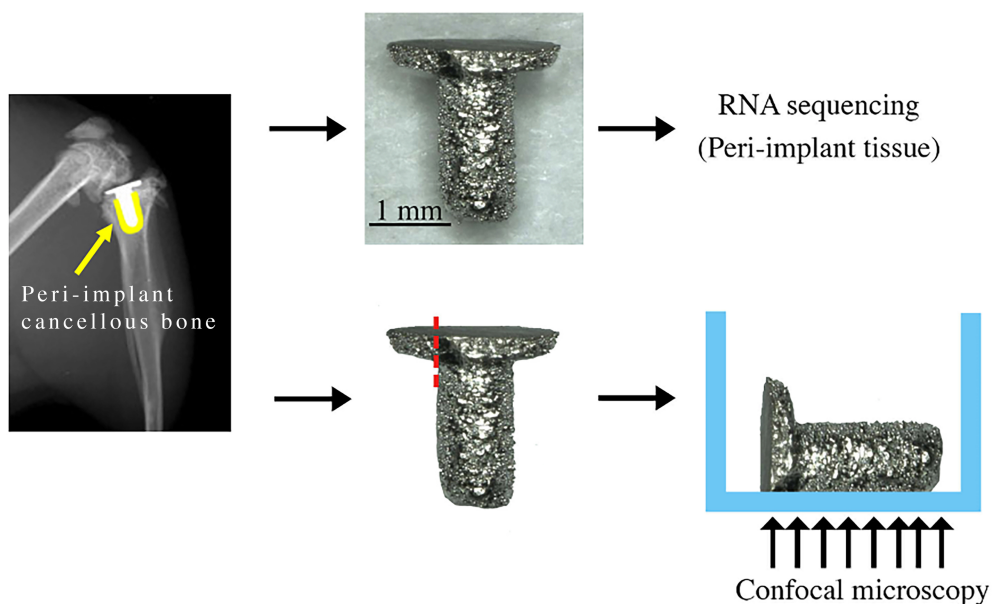


Fig. 1. Peri-implant tissue collection and immunofluorescence staining preparation. The implant was removed from the right tibias. (Yellow = cancellous bone around the implant.) One end of the tibial plateau component of the implant was polished before immunofluorescence staining.

(Fig. 1).^(15,19,23) Mice started weight-bearing with the implanted knee immediately after recovering from anesthesia.

RNA extraction and purification

Mice were euthanized 1 week post-implantation. Right tibias were rapidly dissected to remove soft tissue, fibulae, and malleoli. Implants with attached tissue (peri-implant tissue) were removed from the tibia, and bone marrow was isolated by centrifugation (10,000 g for 30 seconds) using nested tubes. Next, the implant with tissue on its surface and adjacent cancellous bone, collected using a 1 mm biopsy punch, were separately stored in 2 mL pre-filled 2.4 mm metal beads tubes (VWR International, Radnor, PA, USA), and quickly snap-frozen in liquid nitrogen.⁽⁴⁰⁾ The bone specimens were stored at -80°C for later RNA extraction and purification.

Our method of RNA extraction was adapted and modified based on the protocol previously reported by Kelly and colleagues.⁽⁴⁰⁾ RNA isolation from peri-implant tissue was performed using Trizol (Life Technologies, Carlsbad, CA, USA) and RNeasy Mini Kit (Qiagen, Germantown, MD, USA). Briefly, once the samples were removed from -80°C , 1 mL of cold Trizol was immediately added to each sample. Then, the samples were homogenized (TissueLyser II, Qiagen) for 3 minutes at 30 Hz. A total of 200 μL of chloroform was added to the samples and vortexed for 15 seconds. Next, the samples were centrifuged for 15 minutes at 4°C (10,000 g). The aqueous phase, approximately 600 μL , was removed and added to 600 μL of 70% ethanol to precipitate nucleic acids. RNA purification was performed using an RNeasy Mini Kit (Qiagen) according to the manufacturer's instructions, including DNase digestion (RNase-free DNase kit, Qiagen). A final volume of 25 μL was eluted.

RNA purity and quantity were determined using a spectrophotometer (Nanodrop One, Thermo Fisher Scientific, Waltham, MA, USA). In addition, RNA integrity number (RIN) and quality parameters were assessed (2100 Bioanalyzer Instrument, Agilent Technologies, Santa Clara, CA, USA). RNA integrity numbers were 8.3 ± 0.7 and 7.6 ± 0.6 for young and aged mice, respectively. RNA samples with low RIN and quality were discarded from the study.

RNA sequencing

TruSeq RNA Sample Preparation Kits v2 were utilized for cDNA library preparation (Illumina, San Diego, CA, USA).⁽⁴¹⁾ Briefly, poly-A containing mRNA was isolated, converted into cDNA, and end-repaired and ligated to sequencing adapters. The resultant products were column-purified and PCR-enriched to generate final Illumina-compatible libraries (Agencourt AMPure XP, Beckman Coulter, Brea, CA, USA). The libraries from young peri-implant tissues ($n = 6$) and aged peri-implant tissues ($n = 5$) were sequenced by Weill Cornell Medicine Epigenomics Core Facility using a HiSeq2500 with 50-bp single-end reads to a depth of ~ 15 to 25 million reads per sample.

RNA-seq analyses

Read quality assessment and adapter trimming were performed using fastp. Reads that passed quality-control filtering were then mapped to the mouse genome (10 mm) and reads-in-exons were counted against Gencode v27 annotation with STAR aligner.^(42,43) Differential gene expression analysis was performed with edgeR using the quasi-likelihood framework in R environment.

Genes with low expression levels (<3 counts per million [cpm] in at least one group) were filtered from all downstream analyses in initial analyses. To ensure that this relative aggressive filter did not remove interesting low-abundance signatures, we repeated the analyses with 0.3 cpm filter. The Benjamin-Hochberg false discovery rate (FDR) procedure was used to correct for multiple testing.⁽⁴⁴⁾ When the young and aged mice are compared, genes with FDR (corrected p value) less than 0.01 and log₂-fold change greater than 1 were considered differentially expressed. Gene expression changes were evaluated for enrichment of known signaling pathways with the quantitative set analysis for gene expression (QuSAGE) method. Data visualization and downstream analyses were performed in R using a Shiny-driven visualization platform (RNAseq DRAMA) developed at the David Z. Rosensweig Genomics Research Center at the Hospital for Special Surgery (<https://gitlab.com/hssgenomics/Shiny>).

RNA-seq cell type decomposition

To perform bulk RNA-seq cell type decomposition, we used the SCDC algorithm that utilizes cell type-specific gene expression information from single-cell RNA sequencing (scRNA-seq) experiments.⁽⁴⁵⁾ To generate cell type-specific scRNA-seq reference data sets, we extracted raw scRNA count matrices from the Panglao database of scRNA-seq data that covered 2,046,548 cells from 969 experiments/samples that belonged to 119 cell types in mice.⁽⁴⁶⁾ To improve the quality of prediction and decrease the search space, we performed rigorous quality filtering at both the experiment and individual cell levels. We first removed all cells with no assigned cell type. We then removed all individual cells with the total percentage of mitochondrial counts $>5\%$ for cell types found in multiple experiments. We focused only on polyadenylated RNAs and selected 33,979 genes. After filtering, we created a database of 1,837,691 high-quality cells representing 855 experiments and 119 cell types. Finally, we limited the search space to 37 cell types that we expected to encounter in a typical bone-related surgical material (Supplemental Fig. S1). We refer to this assemblage as bone-immune cell set (BICS). One hundred cells were randomly sampled for each cell type from BICS; for seven cell types in BICS that were represented by fewer than 100 cells, we used all cells available. The within-cell-type randomized reference sets were used by SCDC to determine the cell-type proportion for each bulk RNA-seq replicas (two groups, five replicas for aged and six for young mice). The reference resampling was performed 100 times and the median cell-type proportion was determined for each bulk RNA-seq replica and for both young and aged samples overall.

Immunofluorescence staining of peri-implant tissue

To validate the observation of expression of T-cell marker and activation genes in aged mice indicated by RNA-seq, we used immunofluorescence to confirm the presence of T cells at the bone-implant interface. One week post-implantation, right tibias were rapidly dissected, and soft tissue, fibulae, and malleoli were removed. Implants with attached tissue (peri-implant tissue) were removed from the tibia ($n = 3$ per group) (Fig. 1). Then, the implants were polished using Grit 320/P400 sandpaper to remove one end of the tibial plateau. The implants were fixed with 4% paraformaldehyde (PFA) for 1 hour. After 4% PFA was removed, the implants were washed with 1X PBS for 5 minutes and permeabilized with 0.3% Triton X-100 for 15 minutes at room temperature, respectively. Next, the implants were washed

once with 1X PBS for 5 minutes and blocked with 5% donkey serum for 1 hour at room temperature. Subsequently, the primary antibody, CD3 (NBP2-43674, Novus Biologicals, Littleton, CO, USA), was separately diluted in 5% donkey serum (1:100) and incubated overnight at 4°C. After the removal of primary antibody, secondary antibody, Alexa fluor plus 555 donkey anti-mouse IgG secondary antibody (A32773, Invitrogen, Carlsbad, CA, USA), was diluted in 1X PBS (1:400) and applied for 1 hour at room temperature. Then, the implants were washed once with 1X PBS and incubated in DAPI for 10 minutes at room temperature. The implants were then washed once with 1X PBS and placed in 8-well chamber slides (Thermo Fisher Scientific) (Fig. 1). The images were collected as z-stacks at 10× magnification using confocal microscopy (LSM 880, Zeiss, White Plains, NY, USA).

Results

Suppressed induction of Notch, angiogenesis, and Wnt pathways at bone-implant interface tissue in aged mice

To gain insight into how aging affects osseointegration at the bone-implant interface, we performed RNA-seq of implant-associated tissue from old versus young mice 1 week after implantation. This time point corresponds to early osseointegration, where deposition of woven bone overlaps with a resolving inflammatory response.^(15,19,23,33,35,40)

A total of 872 genes were differentially expressed between old and young mice (FDR <0.01, fold change >2), of which 696 were expressed at a higher level in aged mice than in young mice (Fig. 2A; Supplemental Table S1). To assess differences between old and young peri-implant tissue, we performed pathway enrichment analysis using QuSAGE with the MSigDb c2 set of curated pathways. Interestingly, among pathways with elevated gene expression in young mice, we noticed several bone anabolic pathways, including Notch (Fig. 2B, pathways 9, 10, and 12; Supplemental Table S2) and Wnt-related pathways (Fig. 2B, pathway 11). Further inspection of differentially expressed genes revealed that multiple genes in the Notch pathway, including Notch ligands (*Jag1*, *Jag2*, *Dll1*, and *Dll4*), receptors (*Notch3*, *Notch4*), and downstream transcription factors (*Hey1*, *Hey2*, *Heyl*, and *Hes1*) were more highly expressed in young peri-implant tissue (Fig. 2A, upper right quadrant, orange dots and Fig. 2C). Similarly, several Wnt ligand receptors (*Fzd4*, 5, 8, and 9) and Wnt-regulated transcription factors (*Tcf7l1*, *Tcf7l2*, and *Tle2*) were elevated in young mice (Fig. 2A, C). Regarding expression of transcription factors that are important in osteoblast differentiation, *Sp7* (which encodes Osterix) was not affected by aging, whereas *Runx2* was higher in young mice (Fig. 2A). These results show that osseointegration at the implant surface in old mice is characterized by defective activity of the Notch pathway, which is important for both angiogenesis and expansion of bone progenitor cells. Expression of genes of the bone anabolic Wnt pathway during implant osseointegration is also compromised to a lesser extent in aged mice.

Angiogenesis is a process of new blood vessel formation that is promoted by VEGF and Notch signaling^(47–49) and is important for new bone formation, fracture healing, and osseointegration.^(15,50–53) Recent work has implicated specialized Endomucin-high endothelium, which is regulated by the SLIT3/ROBO1 pathway, in bone vascularization and titanium implant integration.^(15,54) Treatment with recombinant SLIT3 improves bone fracture healing and prevents bone loss.^(55–57) Importantly, we observed that both *Slit3*, which appears to be osteoblastic

specific,⁽⁵⁷⁾ and *Robo4*, which can be considered as an endothelial maker,⁽⁵⁷⁾ were more highly expressed in the peri-implant tissue of young mice (Fig. 2A, green dots). Similarly, two VEGF receptors, *Kdr* and *Flt1*, were expressed at a higher level in young mice (Fig. 2A, green dots), further supporting the notion of compromised angiogenesis in old mice.

Increased activation of immune and inflammatory pathways at the bone-implant interface in aged mice

Strikingly, the expression of multiple immune and inflammatory pathways was significantly increased in old relative to young mice, including IL-12-STAT4 signaling (Fig. 2B, pathway 1), innate immune activation (Toll-like receptor [TLR] and IL-1, pathways 2 and 4), and cytokine and chemokine signaling (pathways 3, 5, and 6). Activation of both innate and adaptive immune components was supported by a significant elevation of TLR signaling (pathway 2) and a group of pathways related to T-cell receptor (TCR) signaling (eg, pathway 6). Toll-like receptors are potent activators of inflammatory NF-κB signaling in immune cells and are activated by tissue damage products, whereas TCR signaling is suggestive of activation of lymphocytes.

Expression of the core components of the TCR (*Cd3e*, *Cd3d*, *Cd3g*), co-receptors *Cd4*, *Cd28*, and costimulatory molecules *Cd80/Cd86*, was elevated in aged mice (Fig. 3A, top panel and Fig. 3B). As expression of these molecules typically does not change with cell activation, this result is suggestive of increased infiltration of T cells, including CD4+ T cells, into peri-implant tissue in old mice. Aged peri-implant tissues also exhibited increased expression of *Stat4*, which is induced during differentiation and activation of CD4+ T-helper 1 (Th1) cells, and of *Il12*, a major inducer of Th1 cells. Activated Th1 cells produce IFN-γ and TNF, and, accordingly, expression of *Tnf* and canonical IFN-γ target genes like *Ccl5* was elevated in aged peri-implant tissues (Fig. 3A, middle panel).

Major mediators of innate immunity include the cytokines IL-1, TNF, and TLRs, which activate inflammatory genes via NF-κB signaling. IL-1 is expressed predominantly by innate myeloid cells such as macrophages and dendritic cells, which are also major producers of TNF. The bone-implant interface tissue in aged mice exhibited increased expression of *Il1a*, *Il1b*, and *Tnf* and various downstream inflammatory NF-κB target genes and chemokines such as *Cxcl2*, *Ccl3*, *Ccl4*, and *Ccl8*. Thus, an innate immune response is more strongly activated in aged than young mice in response to bone injury and tibial implantation. TLRs are highly expressed on various immune cells and their expression can increase during cell activation. Strikingly, expression of 8 of 13 known TLRs was elevated in aged relative to young mice (Fig. 3A, bottom panel). This includes TLRs that can sense tissue degradation products such as collagen and fibronectin fragments (TLR2, TLR4) and nucleic acids (TLR7/8) and chromatin proteins (TLR2) released by dying cells.⁽⁵⁸⁾

We then surveyed the relative expression of additional canonical immune cell markers in bone-implant interface tissue (Fig. 3C). In addition to *Cd3d* and *Cd4*, expression of the CD8+ T-cell marker *Cd8a* and of macrophage and DC marker genes *Ilgam*, *Ilgax*, and *Fcgr1* was increased in aged peri-implant tissue, whereas B-cell (*Cd19*) and NK-cell (*Klrb1c*) marker gene expression was comparable in aged and young tissues.

To address more thoroughly how increased expression of inflammatory mediators in aged mice may reflect increased infiltration of immune cells, we performed cell-type decomposition of bulk RNA-seq data using SCDC deconvolution method.⁽⁴⁵⁾

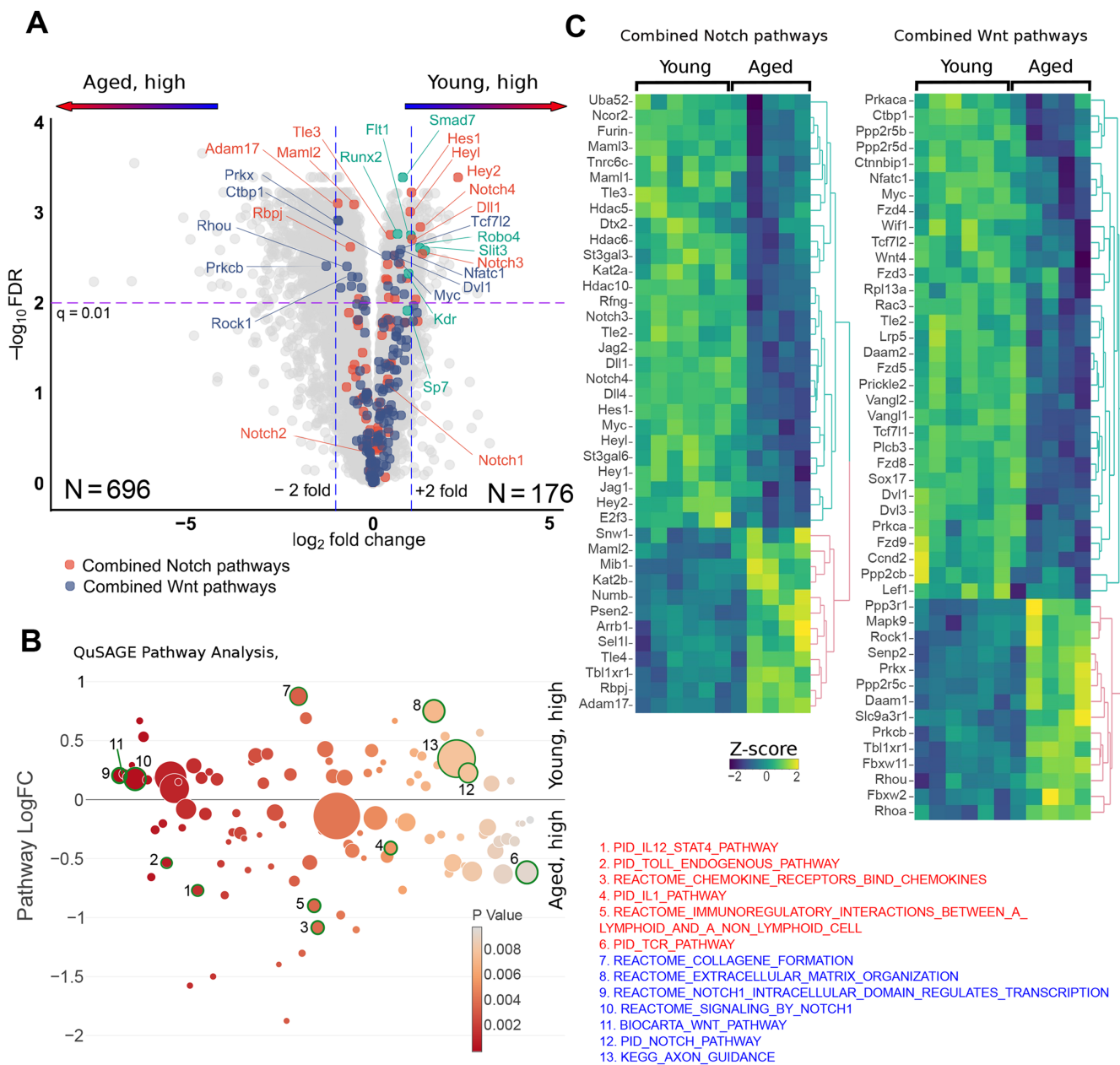


Fig. 2. Differential expression genes involved in bone metabolism and maintenance in the peri-implant tissue from young and aged mice. (A) A volcano plot for gene differential expression analysis of peri-implant tissue from young ($n = 6$) and aged ($n = 5$) mice. Color highlight genes from the combined Notch- and WNT-related pathways indicated at the bottom. Genes involved in angiogenesis are shown in green. (B) QuSAGE differential pathway analysis of the peri-implant tissues from young and aged mice. All pathways with less than 10 genes were discarded and only pathways with p value < 0.01 are shown. The y axis shows pathway-wide log-transformed fold change between young and aged mice and the x axis shows the p value. The size of each circle is proportional to the number of genes in a pathway. Pathways that are upregulated in aged mice (red) and young mice (blue) are listed. (C) Heat maps of standardized log-transformed cpm for differentially expressed genes from the Notch and WNT pathways. The columns represent individual samples from young and aged mice. Clustering of genes was performed using complete linkage method with the Euclidean distance.

SCDC algorithm uses the cell type-specific gene expression reference sets generated from multiple single-cell RNA-seq experiments (see Materials and Methods). Comparison of cell-type composition in peri-implant tissues revealed substantial differences between young and aged mice. In young mice 1 week after surgery, cells expressing osteoblast lineage genes represent the largest proportion of cells in the bulk RNA-seq

samples ($> 50\%$); this is in accord with mobilization of stromal precursors, which differentiate along the osteoblast pathway to lay down bone. Fibroblasts and macrophages were the distant next two common cell types in young peri-implant tissue (Fig. 4A). In aged mice, the proportion of osteoblast-lineage cells contributing to bulk RNA-seq gene expression was decreased considerably (24%), and the macrophages became the largest

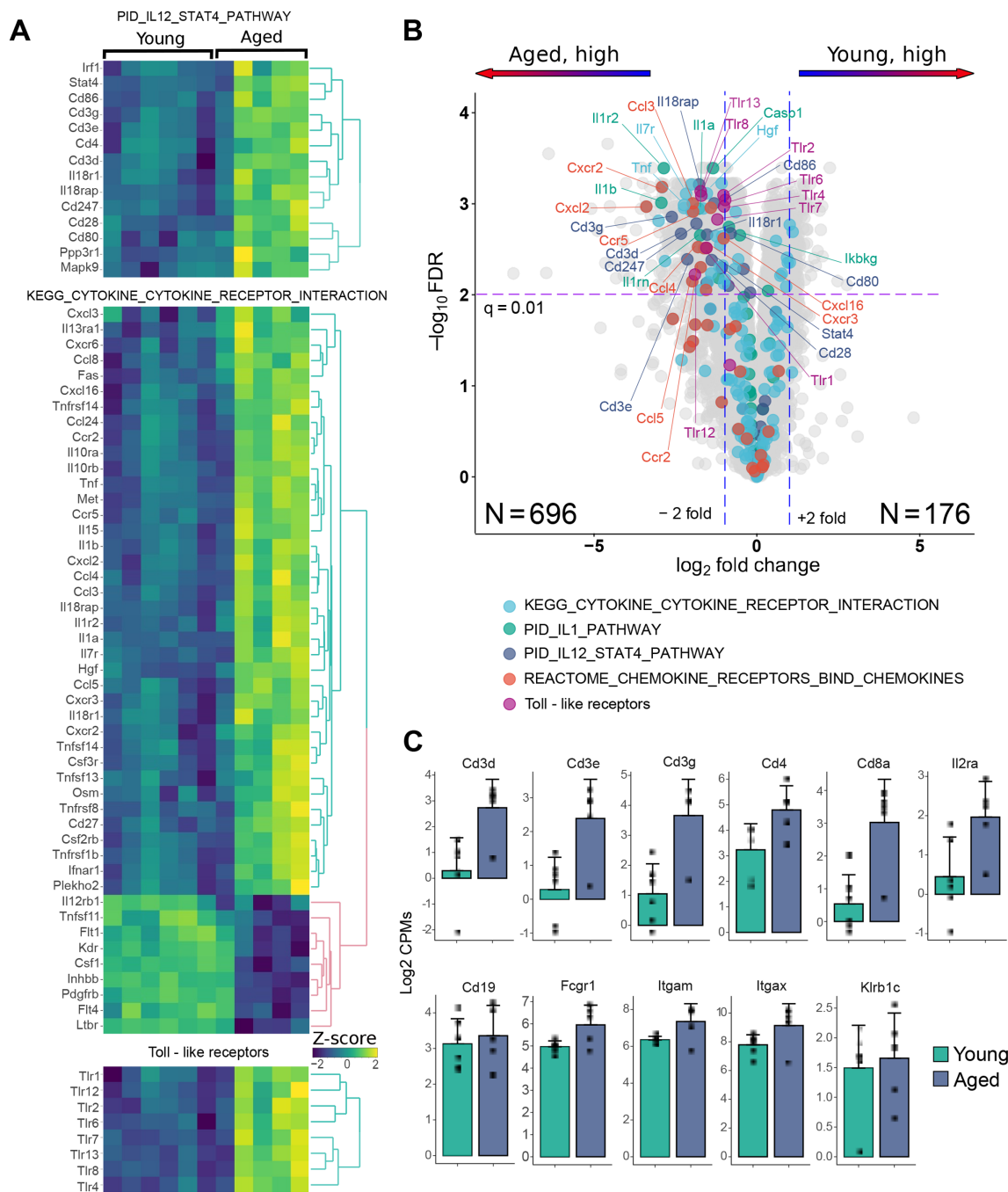


Fig. 3. Differential expression inflammatory genes in the peri-implant tissue from young and aged mice. (A) Heat maps of standardized log-transformed cpm of differentially expressed immune-inflammatory genes from the PID IL12_STAT, KEGG CYTOKINE_CYTOKINE_RECEPTOR_INTERACTION pathways and Toll-like receptors. The columns represent individual samples from young and aged mice. Clustering of genes was performed using complete linkage method with the Euclidean distance. (B) A volcano plot for gene differential expression analysis of peri-implant tissue from young ($n = 6$) and aged ($n = 5$) mice. Color highlight genes from the pathways indicated at the bottom of each panel. (C) Comparison of cell surface marker expression in young and aged maps: T cells—Cd3d, Cd3e, Cd3g, Cd4, Cd8a, Il2ra(Cd25); B cells—Cd19, monocytes/macrophages Fcgr1 (Cd64), Itgam (Cd11b); dendritic cells—Itgax (Cd11c); NK cells—Klrb1c (NK1.1).

contributing cell type (28%). Concomitantly, several other immune cell types were elevated in old compared with young mice (Fig. 4B; Supplemental Fig. S1), although these cell types were present at a much lower level.

Overall, these findings suggest that bone injury and implant insertion elicit increased immune cell infiltration and stronger innate immune response at the bone-implant interface in aged mice relative to young mice.

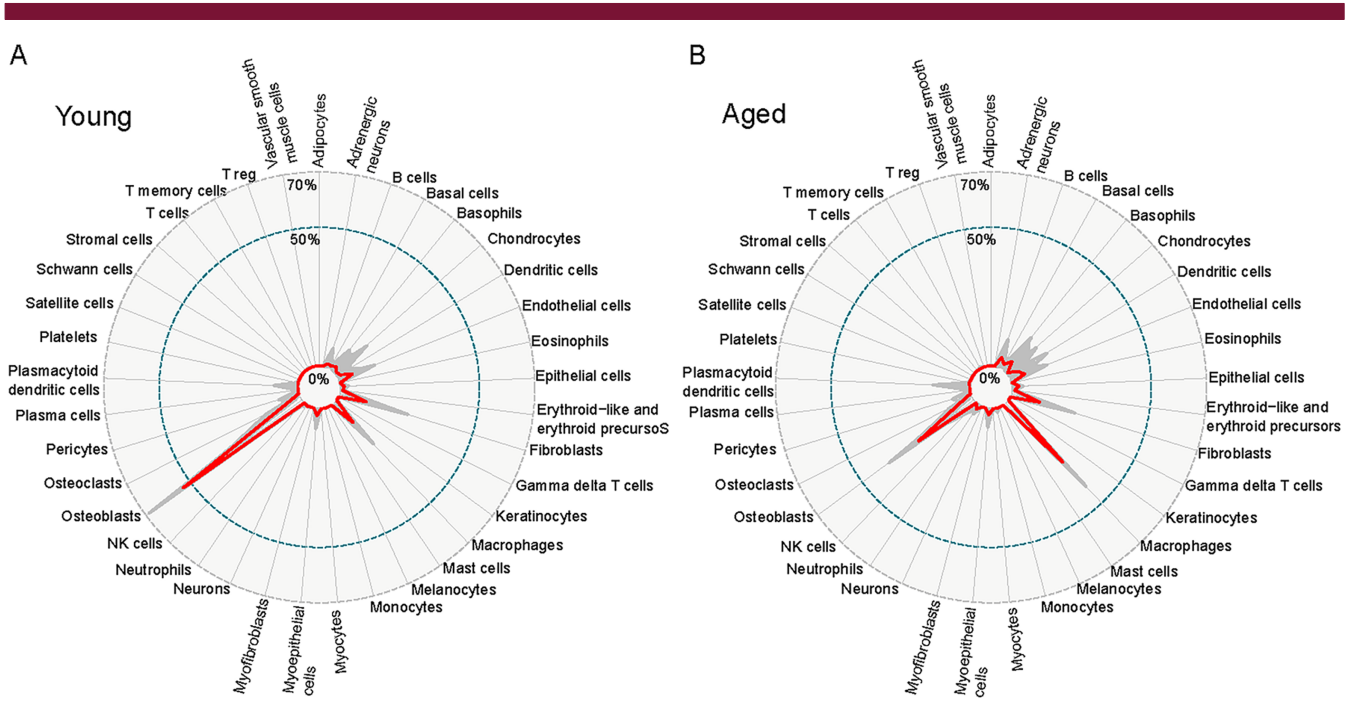


Fig. 4. Cell type decomposition of bulk RNA-seq data from young (A) and aged (B) peri-implant tissue. Cell type composition has been inferred as described in Materials and Methods. The red line represents the median proportion of each cell type from BICS for all bulk RNA-seq replicas and all 100 bulk-to-scRNA-seq reference comparisons. The thin gray lines represent the average proportions of each group (young versus aged) for each cell type from BICS across all the iterations to show the variation in each SCDC proportional output.

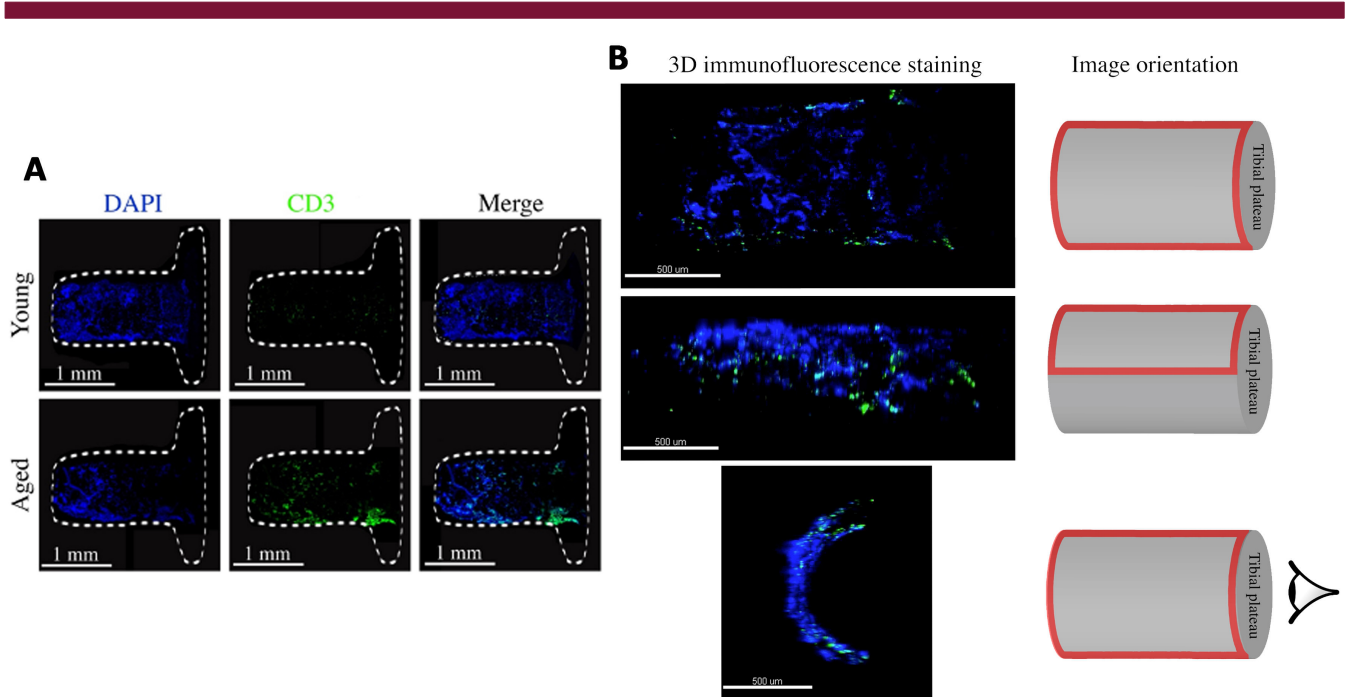


Fig. 5. 3D immunofluorescence staining of the implant surface harvested from young and aged mice. (A) After 1 week post-implantation, the implants were polished, fixed, and stained using alexa fluor plus 555 donkey anti-mouse IgG secondary antibody to detect CD3 (green) and DAPI to label nuclei (blue) (10 \times , z stacks). The white dashed lines represent the outline of the implant. (B) Confocal imaging and image orientation. The red frames indicate the image region.

Similarly, we have additionally performed differential expression and pathway analyses in cancellous bone adjacent to the implant in aged versus young mice (Supplemental Fig. S2A). We noted a highly significant difference in transcripts associated with bile acid and bile salt metabolism pathway (Supplemental Fig. S2A, pathway 1; Supplemental Table S3). This was primarily due to elevated expression of cholesterol 25-hydroxylase (*Ch25h*) (Supplemental Fig. S2B) in aged mice, consistent with age-related differences in cell metabolism. Large differences were also observed in the expression of genes involved in protein secretion and matrisome associated gene sets (pathways 3 and 4), which combine many proteins of extracellular matrix (ECM), ECM-modifying enzymes, and soluble growth factors.⁽⁵⁹⁾ This finding likely reflects basal differences in bone metabolism and response to injury between young and aged mice.

Considering the possibility that interesting low-abundance signatures are removed by using a filter of 3 cpm, we performed additional analyses with a less stringent filter of 0.3 cpm. Despite dramatic increase in the number of genes with low expression, in aged mice, we observed the upregulations of the same immune and inflammatory pathways (Supplemental Fig. S3; Supplemental Tables S4 and S5) as detected with the filter of 3 cpm. In the young mice, in addition to increased expression of Notch, WNT, and ROBO pathways and several pathways related to bone matrix syntheses, we observed the activation of the Hedgehog pathway that also contributes to bone healing (Supplemental Fig. S3, pathways 8, 13).

T-cell infiltration at the bone-implant interface

After the observation of expression of T-cell marker and activation genes (Fig. 3A–C) in aged mice, we wished to confirm the presence of T cells at the bone-implant interface using immunofluorescence microscopy. This is technically challenging as the peri-implant tissue remains attached to the titanium implant after removal of the implant from the tibia. Thus, we developed an approach using confocal microscopy for 3D immunofluorescence imaging of tissue adherent to the implant surface. CD3 staining was readily observed in implant-associated tissue, supporting infiltration of T cells into peri-implant tissue ($n = 3/$ group, Fig. 5).

Discussion

The mechanistic basis for poor osseointegration in elderly patients is not understood, but increased inflammation that occurs with aging (“inflamm-aging”) has been implicated in tissue degeneration and poor healing in other systems.^(60–63) Here, we have extended our clinically relevant, mechanically loaded murine model of TJR through the development of new methods to address the technical challenge of performing transcriptional profiling of the very limited peri-implant bone tissue. Our results reveal age-related decreases in angiogenic and bone anabolic pathways associated with increased immune activation at the site where injured bone integrates with a clinically relevant porous titanium implant. These findings highlight the importance of augmenting angiogenic and bone anabolic pathways in elderly patients undergoing TJR and suggest immune modulation as a novel therapeutic strategy to enhance implant osseointegration.

We performed our studies 1 week post-implantation, when the initial inflammatory response to injury is subsiding and the

bone formation phase is underway.^(15,19,23,33,35) At this phase, increased and sustained inflammation in aged mice mediated by innate immune cytokines such as TNF and IL-1 can suppress osseointegration by augmenting osteoclastogenesis, suppressing osteoblasts directly or via increased production of Wnt pathway inhibitors such as DKK1^(32,64) and compromising the emergence of a preresolution immune response. Innate immune cells are directly activated by tissue damage and degradation products, activate tissue resident cells, and induce production of chemokines that attract additional innate and acquired immune cells from circulation to the site of injury. We unexpectedly observed increased T-cell infiltration and an IFN- γ gene signature in the peri-implant tissue, indicative of IFN- γ production. It is not yet clear whether IFN- γ at the site of osseointegration is produced by CD4+, CD8+, and $\gamma\delta$ T cells or NK cells and how these cells become activated. However, given its role in suppressing fracture repair, bone formation, Notch signaling, and angiogenesis, it is likely IFN- γ contributes to impaired osseointegration in aged mice.^(35,36,65,66)

Our data suggest that pathways for osteogenesis, angiogenesis, and inflammation are activated at the peri-implant site within 1 week after implantation. Aged mice exhibit impaired expression of genes associated with vascular formation and preferential suppression of Notch signaling relative to other anabolic pathways (Wnt, BMP, PTH), suggesting that Notch-mediated osteogenic mechanisms are disproportionately affected by aging. Diminished Notch pathway activity may contribute to decreased osseointegration by decreasing angiogenesis in addition to decreased endochondral and intramembranous ossification.^(67,68) The notion that elevated immune and inflammatory responses in elderly organisms may suppress bone anabolic, or promote resorptive, pathways is consistent with previous reports of decreased fracture healing with age.^(37,69–71)

Typically, histological evaluation of clinical implant samples is performed after patients experience implant failure. The absence of samples from early stage osseointegration failure and successful osseointegration impair our ability to understand the early steps in osseointegration failure. Furthermore, the existence of metal implant in the bone makes sample preparation difficult. Therefore, using our murine model, we developed a novel technique of 3D immunofluorescence staining to analyze the peri-implant (surface) tissue without cutting our specimens. This implant surface staining technique can be utilized to monitor the process of bone formation on the implant surface or identify presence of bacteria in a bone infection animal model. In addition, the approach can be applied to evaluate bone healing on the surface of various implant materials.

Our study has several limitations. The gene expression data analysis was based on mixed cell populations. This approach identifies changes in cell composition based on marker gene expression and cell deconvolution algorithms, but it is more difficult to assess cell activation states and which cell populations are being activated. In addition, this study only evaluated one time point, which does not reflect the entire process of bone healing after implantation. Future studies should focus on finding methods to enhance osteogenesis and angiogenesis and regulate inflammation in elderly patients. Our model can provide a viable platform for preclinical studies. Furthermore, this study opens the possibility that targeting the Notch pathway, promoting angiogenesis, or modulating the immune response at the peri-implant site can enhance osseointegration and improve the outcome of joint replacements in older patients.

Disclosures

All authors state that they have no conflicts of interest.

Acknowledgments

We acknowledge the Weill Cornell Medicine Microscopy and Image Analysis Core Facility for image analysis consulting, the Weill Cornell Medicine Genomics Resources Core Facility and Weill Cornell Medicine Epigenomics Core Facility for nucleic acid quality assessment and RNA sequencing, and the David Z. Rosensweig Genomics Research Center at the Hospital for Special Surgery for RNA sequencing data analyses. The implants were manufactured and donated by Smith & Nephew, Inc. This work was supported by Adult Reconstruction and Joint Replacement (ARJR) Marmor Research Grant from the Hospital for Special Surgery. MBG holds a Career Award for Medical Scientists from the Burroughs Wellcome Fund, awards from the NIH under DP5OD021351 and R01AR075585, and an award from the Pershing Square Sohn Cancer Research Alliance. The Rosensweig Genomics Center is supported by The Tow Foundation. LBI was supported by NIH grants DE019420 and AI044938. XY was supported by grant UL1 TR000457 of the Clinical and Translational Science Center at Weill Cornell Medicine and Feldstein Medical Foundation.

Authors' roles: Each author participated in reviewing and editing the manuscript and other aspects of the project. KT: data curation, methodology, formal analysis, and writing the original draft. GJ: data curation and methodology. YC: formal analysis, data vitalization, and writing the original draft. MC: formal analysis and data vitalization. UA: conceptualization and methodology. VJS: data curation and methodology. MBG: conceptualization. LBI: conceptualization and writing original draft. MPGB: funding acquisition, resources, and conceptualization. XY: conceptualization, project administration and supervision, and writing original draft.

Peer Review

The peer review history for this article is available at <https://publons.com/publon/10.1002/jbmr.4.10535>.

References

1. Sloan M, Premkumar A, Sheth NP. Projected volume of primary total joint arthroplasty in the U.S., 2014 to 2030. *J Bone Joint Surg Am.* 2018; 100(17):1455-1460.
2. Dalury DF. Cementless total knee arthroplasty: current concepts review. *Bone Joint J.* 2016;98-B(7):867-873.
3. Giebaly DE, Twaij H, Ibrahim M, Haddad FS. Cementless hip implants: an expanding choice. *Hip Int.* 2016;26(5):413-423.
4. Delanois RE, Mistry JB, Gwam CU, Mohamed NS, Choksi US, Mont MA. Current epidemiology of revision total knee arthroplasty in the United States. *J Arthroplasty.* 2017;32(9):2663-2668.
5. Gwam CU, Mistry JB, Mohamed NS, et al. Current epidemiology of revision total hip arthroplasty in the United States: national inpatient sample 2009 to 2013. *J Arthroplasty.* 2017;32(7):2088-2092.
6. Albrektsson T, Albrektsson B. Osseointegration of bone implants. A review of an alternative mode of fixation. *Acta Orthop Scand.* 1987; 58(5):567-577.
7. Trindade R, Albrektsson T, Galli S, Prgomet Z, Tengvall P, Wennerberg A. Osseointegration and foreign body reaction: titanium implants activate the immune system and suppress bone resorption during the first 4 weeks after implantation. *Clin Implant Dent Relat Res.* 2018;20(1):82-91.
8. Yang C, Han X, Wang J, et al. Cemented versus uncemented femoral component total hip arthroplasty in elderly patients with primary osteoporosis: retrospective analysis with 5-year follow-up. *J Int Med Res.* 2019;47(4):1610-1619.
9. Finnilä S, Moritz N, Svedström E, Alm JJ, Aro HT. Increased migration of uncemented acetabular cups in female total hip arthroplasty patients with low systemic bone mineral density. *Acta Orthop.* 2016;87(1):48-54.
10. Aro HT, Alm JJ, Moritz N, Mäkinen TJ, Lankinen P. Low BMD affects initial stability and delays stem osseointegration in cementless total hip arthroplasty in women: a 2-year RSA study of 39 patients. *Acta Orthop.* 2012;83(2):107-114.
11. Zaid MB, O'Donnell RJ, Potter BK, Forsberg JA. Orthopaedic osseointegration: state of the art. *J Am Acad Orthop Surg.* 2019;27(22):e977-e985.
12. Fahlgren A, Yang X, Ciani C, et al. The effects of PTH, loading and surgical insult on cancellous bone at the bone-implant interface in the rabbit. *Bone.* 2013;52(2):718-724.
13. van der Meulen MCH, Morgan TG, Yang X, et al. Cancellous bone adaptation to in vivo loading in a rabbit model. *Bone.* 2006;38(6): 871-877.
14. Grosso MJ, Courtland HW, Yang X, et al. Intermittent PTH administration and mechanical loading are anabolic for periprosthetic cancellous bone. *J Orthop Res.* 2015;33(2):163-173.
15. Ji G, Niu Y, Xu R, et al. Vascular endothelial growth factor pathway promotes osseointegration and CD31hiEMCNhi endothelium expansion in a mouse tibial implant model: an animal study. *Bone Joint J.* 2019;101-B(7 Suppl C):108-114.
16. Van Der Meulen MCH, Yang X, Morgan TG, Bostrom MPG. The effects of loading on cancellous bone in the rabbit. *Clin Orthop Relat Res.* 2009;467(8):2000-2006.
17. Pearce AI, Richards RG, Milz S, Schneider E, Pearce SG. Animal models for implant biomaterial research in bone: a review. *Eur Cells Mater.* 2007;13:1-10.
18. Sumner DR, Turner TM, Urban RM. Animal models relevant to cementless joint replacement. *J Musculoskelet Neuronal Interact.* 2001;1(4):333-345.
19. Vertesich K, Sosa BR, Niu Y, et al. Alendronate enhances osseointegration in a murine implant model. *J Orthop Res.* 2021;39(4):719-726.
20. Willie BM, Yang X, Kelly NH, et al. Cancellous bone osseointegration is enhanced by in vivo loading. *Tissue Eng Part C Methods.* 2010;16(6): 1399-1406.
21. Willie BM, Yang X, Kelly NH, et al. Osseointegration into a novel titanium foam implant in the distal femur of a rabbit. *J Biomed Mater Res Part B Appl Biomater.* 2010;92(2):479-488.
22. Yang X, Willie BM, Beach JM, Wright TM, Van Der Meulen MCH, Bostrom MPG. Trabecular bone adaptation to loading in a rabbit model is not magnitude-dependent. *J Orthop Res.* 2013;31(6): 930-934.
23. Yang X, Ricciardi BF, Dvorzhinskiy A, et al. Intermittent parathyroid hormone enhances cancellous osseointegration of a novel murine tibial implant. *J Bone Joint Surg Am.* 2015;97(13):1074-1083.
24. Wancket LM. Animal models for evaluation of bone implants and devices: comparative bone structure and common model uses. *Vet Pathol.* 2015;52(5):842-850.
25. Claes L, Recknagel S, Ignatius A. Fracture healing under healthy and inflammatory conditions. *Nat Rev Rheumatol.* 2012;8(3):133-143.
26. Einhorn TA, Gerstenfeld LC. Fracture healing: mechanisms and interventions. *Nat Rev Rheumatol.* 2015;11(1):45-54.
27. Lorenzo J, Horowitz M, Choi Y. Osteoimmunology: interactions of the bone and immune system. *Endocr Rev.* 2008;29(4):403-440.
28. Tsukasaki M, Takayanagi H. Osteoimmunology: evolving concepts in bone-immune interactions in health and disease. *Nat Rev Immunol.* 2019;19(10):626-642.
29. Takayanagi H. Osteoimmunology and the effects of the immune system on bone. *Nat Rev Rheumatol.* 2009;5(12):667-676.

30. Zhao B, Ivashkiv LB. Negative regulation of osteoclastogenesis and bone resorption by cytokines and transcriptional repressors. *Arthritis Res Ther*. 2011;13(4):1-10.
31. Yu M, Malik Tyagi A, Li JY, et al. PTH induces bone loss via microbial-dependent expansion of intestinal TNF+ T cells and Th17 cells. *Nat Commun*. 2020;11(1):1-17.
32. Gravallese E, Schett G. Bone erosion in rheumatoid arthritis: mechanisms, diagnosis and treatment. *Nat Rev Rheumatol*. 2014;8(11):656-664.
33. Bragdon B, Lybrand K, Gerstenfeld L. Overview of biological mechanisms and applications of three murine models of bone repair: closed fracture with intramedullary fixation, distraction osteogenesis, and marrow ablation by reaming. *Curr Protoc Mouse Biol*. 2015;5(1):21-34.
34. Ono T, Okamoto K, Nakashima T, et al. IL-17-producing $\gamma\delta$ T cells enhance bone regeneration. *Nat Commun*. 2016;7:1-9.
35. Ono T, Takayanagi H. Osteoimmunology in bone fracture healing. *Curr Osteoporos Rep*. 2017;15(4):367-375.
36. Schlundt C, Reinke S, Geissler S, et al. Individual effector/regulator T cell ratios impact bone regeneration. *Front Immunol*. 2019;10(Aug):1-14.
37. Vi L, Baht GS, Soderblom EJ, et al. Macrophage cells secrete factors including LRP1 that orchestrate the rejuvenation of bone repair in mice. *Nat Commun*. 2018;9(1):5191.
38. Yahara Y, Barrientos T, Tang YJ, et al. Erythromyeloid progenitors give rise to a population of osteoclasts that contribute to bone homeostasis and repair. *Nat Cell Biol*. 2020;22(1):49-59.
39. Tyagi AM, Yu M, Darby TM, et al. The microbial metabolite butyrate stimulates bone formation via T regulatory cell-mediated regulation of WNT10B expression. *Immunity*. 2018;49(6):1116-1131.e7.
40. Kelly NH, Schimenti JC, Patrick Ross F, van der Meulen MCH. A method for isolating high quality RNA from mouse cortical and cancellous bone. *Bone*. 2014;68:1-5.
41. Ayturk UM, Jacobsen CM, Christodoulou DC, et al. An RNA-seq protocol to identify mRNA expression changes in mouse diaphyseal bone: applications in mice with bone property altering Lrp5 mutations. *J Bone Miner Res*. 2013;28(10):2081-2093.
42. Chen S, Zhou Y, Chen Y, Gu J. Fastp: an ultra-fast all-in-one FASTQ preprocessor. *Bioinformatics*. 2018;34(17):i884-i890.
43. Dobin A, Davis CA, Schlesinger F, et al. STAR: ultrafast universal RNA-seq aligner. *Bioinformatics*. 2013;29(1):15-21.
44. Benjamini Y, Hochberg Y. Controlling the false discovery rate: a practical and powerful approach to multiple testing. *J R Stat Soc Ser B*. 1995;57(1):289-300.
45. Dong M, Thennavan A, Urrutia E, et al. SCDC: bulk gene expression deconvolution by multiple single-cell RNA sequencing references. *Brief Bioinform*. 2021;22(1):416-427.
46. Franzén O, Gan LM, Björkegren JLM. PanglaoDB: a web server for exploration of mouse and human single-cell RNA sequencing data. *Database (Oxford)*. 2019;2019:baz046.
47. Hankenson KD, Dishowitz M, Gray C, Schenker M. Angiogenesis in bone regeneration. *Injury*. 2011;42(6):556-561.
48. Luo Z, Shang X, Zhang H, et al. Notch signaling in osteogenesis, osteoclastogenesis, and angiogenesis. *Am J Pathol*. 2019;189(8):1495-1500.
49. Ramasamy SK, Kusumbe AP, Wang L, Adams RH. Endothelial notch activity promotes angiogenesis and osteogenesis in bone. *Nature*. 2014;507(7492):376-380.
50. Hu K, Olsen BR. Vascular endothelial growth factor control mechanisms in skeletal growth and repair. *Dev Dyn*. 2017;246(4):227-234.
51. Lin GL, Hankenson KD. Integration of BMP, Wnt, and notch signaling pathways in osteoblast differentiation. *J Cell Biochem*. 2011;112(12):3491-3501.
52. Raines AL, Olivares-Navarrete R, Wieland M, Cochran DL, Schwartz Z, Boyan BD. Regulation of angiogenesis during osseointegration by titanium surface microstructure and energy. *Biomaterials*. 2010;31(18):4909-4917.
53. Raines AL, Berger MB, Patel N, Hyzy SL, Boyan BD, Schwartz Z. VEGF-A regulates angiogenesis during osseointegration of Ti implants via paracrine/autocrine regulation of osteoblast response to hierarchical microstructure of the surface. *J Biomed Mater Res Part A*. 2019;107(2):423-433.
54. Kusumbe AP, Ramasamy SK, Adams RH. Coupling of angiogenesis and osteogenesis by a specific vessel subtype in bone. *Nature*. 2014;507(7492):323-328.
55. Li N, Inoue K, Sun J, et al. Osteoclasts are not a source of SLIT3. *Bone Res*. 2020;8(1):11-19.
56. Paul JD, Coulombe KLK, Toth PT, et al. SLIT3-ROBO4 activation promotes vascular network formation in human engineered tissue and angiogenesis in vivo. *J Mol Cell Cardiol*. 2013;64:124-131.
57. Xu R, Yallowitz A, Qin A, et al. Targeting skeletal endothelium to ameliorate bone loss. *Nat Med*. 2018;24(6):823-833.
58. Aucott H, Sowinska A, Harris HE, Lundback P. Ligation of free HMGB1 to TLR2 in the absence of ligand is negatively regulated by the C-terminal tail domain. *Mol Med*. 2018;24(1):1-10.
59. Hynes RO, Naba A. Overview of the matrisome—an inventory of extracellular matrix constituents and functions. *Cold Spring Harb Perspect Biol*. 2012;4(1):a004903.
60. Bahney CS, Zondervan RL, Allison P, et al. Cellular biology of fracture healing. *J Orthop Res*. 2019;37(1):35-50.
61. Baht GS, Vi L, Alman BA. The role of the immune cells in fracture healing. *Curr Osteoporos Rep*. 2018;16(2):138-145.
62. Clark D, Nakamura M, Miclau T, Marcucio R. Effects of aging on fracture healing. *Curr Osteoporos Rep*. 2017;15(6):601-608.
63. Goldberg EL, Dixit VD. Drivers of age-related inflammation and strategies for healthspan extension. *Immunity Rev*. 2015;265(1):63-74.
64. Diarra D, Stolina M, Polzer K, et al. Dickkopf-1 is a master regulator of joint remodeling. *Nat Med*. 2007;13(2):156-163.
65. Hu X, Chung AY, Wu I, et al. Integrated regulation of toll-like receptor responses by notch and interferon- γ pathways. *Immunity*. 2008;29(5):691-703.
66. Ivashkiv LB. IFN γ : signalling, epigenetics and roles in immunity, metabolism, disease and cancer immunotherapy. *Nat Rev Immunol*. 2018;18(9):545-558.
67. Dishowitz MI, Terkhorn SP, Bostic SA, Hankenson KD. Notch signaling components are upregulated during both endochondral and intramembranous bone regeneration. *J Orthop Res*. 2012;30(2):296-303.
68. Wang C, Inzana JA, Mirando AJ, et al. NOTCH signaling in skeletal progenitors is critical for fracture repair. *J Clin Invest*. 2016;126(4):1471-1481.
69. Gibon E, Lu L, Goodman SB. Aging, inflammation, stem cells, and bone healing. *Stem Cell Res Ther*. 2016;7(1):1-7.
70. Hebb JH, Ashley JW, McDaniel L, et al. Bone healing in an aged murine fracture model is characterized by sustained callus inflammation and decreased cell proliferation. *J Orthop Res*. 2018;36(1):149-158.
71. Josephson AM, Bradaschia-Correa V, Lee S, et al. Age-related inflammation triggers skeletal stem/progenitor cell dysfunction. *Proc Natl Acad Sci*. 2019;116(14):6995-7004.